

USE OF ALKANE MONOLAYER TEMPLATES TO MODIFY THE STRUCTURE OF ALKYL ETHER MONOLAYERS ON HIGHLY ORDERED PYROLYTIC GRAPHITE

2.1 Overview

Scanning tunneling microscopy (STM) has been used to investigate the structure of pure and mixed monolayers formed by adsorption of long-chain alkanes and/or ethers on highly ordered pyrolytic graphite. Application of a pure phenyloctane solution of simple alkanes, such as tritriacontane, $\text{CH}_3(\text{CH}_2)_{31}\text{CH}_3$, produced a monolayer within which the individual molecular axes were oriented perpendicular to the lamellar axes. In contrast, a pure solution of symmetrical long-chain ethers, such as di-*n*-hexadecylether, $\text{CH}_3(\text{CH}_2)_{15}\text{O}(\text{CH}_2)_{15}\text{CH}_3$, produced a monolayer within which the molecular axes were oriented at an angle of $\approx 65^\circ$ relative to the lamellar axes. The compositions of the overlying solutions were then gradually changed either from pure alkanes to nearly pure ethers, or from pure ethers to nearly pure alkanes. When ethers replaced alkanes in the monolayer, the ethers conformed to the orientation within the existing alkane layer, rather than adopting the characteristic orientation of pure ether monolayers. However, when alkanes were incorporated into monolayers that had been formed from pure ether solutions, the orientation of the molecules within the monolayer converted to that characteristic of pure alkanes. Alkane monolayers thus acted as templates for subsequent ether layers, but ether monolayers did not act as templates for alkane layers.

2.2 Introduction

Long-chain alkanes in solution spontaneously form stable, ordered monolayers on a number of surfaces, including graphite, MoS_2 , and WS_2 .¹ This phenomenon is relevant to the fields of separation, adhesion, lubrication, catalysis, and corrosion-resistance. The

alkane monolayers can be observed using a scanning tunneling microscope (STM) when an atomically flat surface, such as highly ordered pyrolytic graphite (HOPG), is used as a substrate.²⁻⁴ STM observations have routinely shown the formation of single, ordered, alkane monolayer domains $> 10,000 \text{ nm}^2$ in area. Because alkane monolayers can easily cover surfaces in a highly ordered manner, such monolayers are potentially useful for nanometer-scale surface patterning and for the production of novel materials. The formation of these monolayers is driven by favorable van der Waals and hydrogen bonding interactions between adsorbed molecules, rather than by surface-adsorbate interactions. As a result, the organization of molecules within these layers is typically determined by the structure of the molecules as well as by their functional groups.⁵⁻⁸ The inability to control the manner in which a given molecule will orient within a monolayer has led to the development of two auxiliary methods for generating more intricate monolayer patterns: the use of solutions containing a mixture of molecules, and of molecules with elaborate or chiral structures.⁹⁻¹⁵

The question of interest in this work was whether the structure of the overlayer formed by a given molecule could be influenced, and in fact templated, by the deliberate prior formation of a monolayer having a different structure. Such behavior would enable manipulation of the structure of the resulting overlayers by prior chemical templating of the surface with monolayers having a structure of interest, constituting a form of overlayer lithography. Since the structures of alkane and ether monolayers are determined by low-energy van der Waals interactions, a monolayer structural template that causes only a limited change to these interactions would produce a monolayer close in energy to that of the original structure. For a templating process to be observable, the structure of the overlayer formed using a template must be close in energy to the structure formed without a template, and one of the two structures must be metastable.

We report herein the results of a series of experiments in which we have examined the structures of monolayers produced by adsorption of molecules onto a pristine substrate and the structures formed by substitution of the molecules into a preexisting monolayer having

a distinctly different overlayer structure. Specifically, straight-chain alkanes and ethers have been investigated because they are known to form differently structured lamellate monolayers on HOPG which are stable and can be imaged by STM for at least several days after their formation. The direct application of a solution of a single alkane, such as tritriacontane, $\text{CH}_3(\text{CH}_2)_{31}\text{CH}_3$, in phenyloctane produces a monolayer in which the alkanes are in registry and thus have their individual molecular axes oriented perpendicular to the lamellar axes of the monolayer. In contrast, a phenyloctane solution of a symmetrical long-chain ether, such as di-*n*-hexadecylether, $\text{CH}_3(\text{CH}_2)_{15}\text{O}(\text{CH}_2)_{15}\text{CH}_3$, produces a monolayer in which each ether molecule is offset from its neighbors.^{16,17} This offset produces an angle of $\approx 65^\circ$ between the molecular and lamellar axes.¹⁸ Alkane–ether pairs having the same molecular lengths were therefore selected for study. Due to functional group-related differences in tunneling contrast, alkanes and ethers are distinguishable in STM images that exhibit atomic resolution. Thus, the composition of the resulting overlayer could be determined as a function of the relative concentrations of alkanes and ethers in the overlying solution whenever imaging conditions were ideal. In our work, the compositions of the overlying solutions were changed either from pure alkane to nearly pure ether solutions, or from pure ether to nearly pure alkane solutions. The structures of the resulting overlayers were then investigated by in-situ STM experiments.

2.3 Experimental details

Experiments were performed with three length-matched (in their all *trans*- configuration) pairs of alkanes and ethers: nonacosane and di-*n*-tetradecylether; tritriacontane and di-*n*-hexadecylether; and heptatriacontane and di-*n*-octadecylether (all from TCI America, > 95% purity). Table 2.1 lists the full chemical formulas and abbreviations for each of these compounds. Pure solutions of each of the six compounds were prepared using phenyloctane (Acros, 99% pure) as the solvent. The solvent was approximately saturated with solute at room temperature, and the solutions were filtered before use. The concentrations of the final solutions were determined using an HP 6890 gas chromatograph equipped with a flame ionization detector, with 1-bromohexadecane (Aldrich) as an

internal standard. The solubilities were determined to be: C29, 23 mM; C33, 4.5 mM; C37, 2.0 mM; E29, 75 mM; E33, 71 mM; and E37, 4.8 mM. Hence, the solubility of the ethers exceeded that of the alkanes, and the solubility decreased with increasing chain length. For each length-matched pair of alkanes and ethers, mixed composition solutions were prepared by mixing volumes of the two component solutions in 80:20, 60:40, 40:60, and 20:80 ratios.

STM images were obtained under ambient laboratory conditions using a Digital Instruments (Veeco) Nanoscope III ECSTM controlled by Nanoscope software version 5.12r2. Tips were mechanically cut from 80:20 Pt/Ir wire. A real-time plane-fitting function was applied to the images while scanning. No additional image corrections were used. Each image consisted of 512 sample scan lines. STM images of pure monolayers were obtained under a drop of the appropriate phenyloctane solution that had been placed on a piece of freshly cleaved HOPG. After \approx 30–45 min, a drop of the length-matched mixed solution having the largest concentration of the species already present on the surface was then added to the cell. For example, after imaging a monolayer formed from a pure C29 solution, 5 μ L of an 80:20 C29/E29 mixed solution was added to the cell. STM images of the resulting monolayer were then obtained after \approx 30–45 min, to allow some time for equilibration of the mixture. The composition of the overlying solution was altered over several steps using the mixed solutions, to ultimately greatly favor the second component of the length-matched mixture. With C29 and E29 for example, after gradually reducing the concentration of C29 in the overlying solution, a few portions of pure E29 solution were added to the overlying solution, to further eliminate C29 from the system. STM images were collected throughout the course of the experiments. Tunneling tips were not changed during experiments, to avoid mechanically disturbing the monolayers.

2.4 Results

Figure 2.1 shows representative STM images of monolayers formed from a phenyloctane solution that contained only an alkane or ether. The orientations of molecules in the lamella of the pure monolayers were consistent with expectations. The alkanes were

oriented with their molecular axes perpendicular to the lamellar axes, whereas the ethers were oriented with their molecular axes at an angle of $\approx 65^\circ$ with respect to the lamellar axes (Figure 2.2). The characteristic monolayer structures of alkanes and ethers shown in Figure 1 were observed for each of the alkanes and ethers studied herein. Table 2.2 lists the unit cell dimensions measured in pure monolayers of each molecule. Although some thermal drift was evident during scanning, its effect was minimal and the drift did not affect the interpretation of the images. The molecules having longer chain lengths formed monolayers more readily than those having shorter chain lengths, and alkane monolayers generally formed more readily than monolayers of the identical chain-length ether, consistent with adsorption isotherm data.^{19,20} The expected functional group STM constant-current tunneling contrast was also observed, with ethers exhibiting a dark contrast region around the C-O-C functionality relative to the alkanes or relative to the alkyl groups of the long-chain ethers.¹⁶⁻¹⁸

As alkanes were added to the overlying ether solution and incorporated into an initially pure ether monolayer, the orientation of all of the molecules within the resulting monolayer was observed to change from 65° to 90° . This transition occurred while the mole fraction of ethers was still high (0.90) in the contacting solution. During the transition, the observed mixed-molecular domains were predominantly composed of ether molecules. At any given time in the transition period, the orientation of molecules within domains was not uniform over the entire sample. Some of the domains imaged during the transition period exhibited molecules oriented at 65° , other domains contained molecules oriented at 90° , and still others were composed of molecules oriented at intermediate angles relative to the lamellar axis. The transition period lasted about 15 min, after which time all of the observed mixed-monolayer domains exhibited the 90° orientation. In contrast, when ethers were added to the overlying solution and incorporated into an initially pure alkane monolayer, the perpendicular molecular orientation of molecules in the initial monolayer was retained in the resulting ether-dominated monolayer, even when relatively high mole fractions (> 0.92) of ethers were in the contacting solution (Figure 2.3 and Figure 2.4). The orientation of the initial alkane monolayer was preserved even when the mole fraction of the ether in the

solution well exceeded that at which the transition from 65° to 90° had been observed when alkanes were added to the ether solution. The ether monolayers that were formed from an alkane template exhibited domains of dimensions similar to those of the template and were stable over time. For example, a monolayer left undisturbed overnight that was predominantly E29, formed through replacement of a C29 monolayer, exhibited ether molecules in the perpendicular orientation despite the overlying solution having a 0.94 mole fraction of the ether. Thus two different stable surface structures were observed for monolayers with the same alkane/ether overlayer concentration. The orientation of an alkane template was preserved by predominately ether monolayers at ether concentrations (≥ 0.92 mole fraction) higher than the transition from ether to alkane orientation observed by replacement of ethers with alkanes (0.90 mole fraction ether). For all observed domains, the molecules within the templated monolayers were found to have a consistent orientation relative to the lamellar axes. The surface structures that were observed were determined by whether they had been reached from the pure ether or pure alkane monolayer starting points.

In many of the mixed-composition monolayers, the functional group STM contrast ratio between ethers and alkanes allowed identification of which molecules were ethers and which were alkanes. However, it was not possible to unambiguously identify every molecule in a monolayer, particularly when the concentrations of the two species in the monolayer were similar. When a single molecule of one species was positioned between two molecules of the other species, it was generally not possible to reliably identify the center molecule. Additional difficulties with identification of individual molecule types resulted from an occasional slight loss of resolution during the hours needed for an individual experiment, resulting in images that allowed reliable determination of the orientation of the molecules, but not of the individual molecular species, within each lamella. For these reasons, we have not quantified the compositions of the mixed monolayers from our STM images, but instead report the composition of the overlying solutions that were present when an image of a monolayer was collected. Despite these difficulties, many of the STM images of mixed monolayers were sufficiently clear to

indicate that the composition of the mixed monolayers appeared to consistently reflect, and change with, the composition of the overlying solution. At a given mole fraction of ether to alkane in solution, the composition of the resulting monolayer was approximately independent of whether the alkane or ether was initially present on the surface, even though the structure of the overlayer was clearly a function of the species initially present on the surface.

2.5 Discussion

Molecules of a pure alkane or ether in these physisorbed monolayers are in pseudo-equilibrium with the molecules dissolved in the overlying solution, as a result of molecular exchange between the monolayer and the solution. The residence time for an individual alkane molecule in a monolayer at 22° C has been measured to be 2–5 s.²¹ Upon addition to the solution, a second molecular species can form a separate monolayer phase or can incorporate into the existing monolayer by filling the spaces created by molecules that have desorbed from the surface.^{21,22} The data presented herein indicate that a monolayer initially composed of alkanes can act as a template for the exchanged ether molecules.

In monolayers comprised of long-chain alkanes, adjacent molecules experience favorable van der Waals interactions, with the number of such interactions proportional to the length of the alkane chain. These interactions are maximized when the monolayers assemble with the molecules in registry having their molecular axes perpendicular to their lamellar axes as depicted in Figure 2.1b.^{23,24} In contrast, for ether monolayers, the 65° angle between the molecular and lamellar axes reflects the need to minimize the repulsions between adjacent oxygen atoms by offsetting the molecules by two carbon atoms relative to each other (Figure 2.2b). This orientation results in the loss of favorable van der Waals interactions and thus results in weaker adsorption of the ether than of the length-matched alkane.

By adopting the structure of the ether template, alkanes would be forced into an energetically unfavorable orientation, losing favorable van der Waals interactions without obtaining any offsetting favorable interactions or avoided repulsions. The heat of

adsorption for long-chain alkanes in full registry within monolayers has been measured as increasing by $\approx 2 \text{ kcal mol}^{-1}$ with each carbon added to the length of the chain.¹⁹ The ether template structure would force the alkane molecules into positions where two carbons at each end of each molecule would lose registry with the neighboring molecules. We expect the energy cost of these lost interactions to be comparable to losing up to four carbons from the length of the chain, a cost of $\approx 8 \text{ kcal mol}^{-1}$. This cost is thus too great to allow the alkanes to conform to the 65° orientation of the ether monolayers. The incorporation of almost any alkane molecules into the adsorbed overlayer therefore results in an alteration of the monolayer structure, and the loss of the ether template. In contrast, when ethers substitute into alkane monolayers, the ether molecules are forced into the perpendicular arrangement of the monolayer template. At low concentrations of ether on the surface, few ether–ether pairs exist, so there are few unfavorable oxygen–oxygen interactions, and the structure is stable with the 90° arrangement. However, the STM data indicate that a mixed overlayer that is compositionally $> 50\%$ ether, which clearly has a significant number of ether–ether neighbors, also retains the 90° structure when formed from an alkane template. In the templated mixed alkane/ether monolayer, the energy increase due to the oxygen–oxygen repulsion is offset by the addition of the favorable van der Waals interactions. This energy offset apparently allows the ether molecules to conform to the orientation of the alkane monolayer template. Because a pure ether monolayer does not adopt the 90° orientation, the oxygen–oxygen repulsion must be unfavorable by approximately 8 kcal mol^{-1} . Although we have not calculated the energy of the 65° ether orientation observed for pure solutions or the energy of the perpendicular orientation obtained by replacement of an alkane template, the stability of the templated ether overlayer suggests that the energies of these two structures are comparable. This suggestion is also supported by the observation of an orthorhombic crystalline polymorphism of E33 that appeared to be continuously co-soluble with C33.²⁷ The orthorhombic polymorphism of E33 is a three-dimensional analog to an ether monolayer formed from an alkane template, having ethers arranged with their molecular axes perpendicular to the lamellar axes.

Because it was difficult to distinguish between the ethers and alkanes with certainty when the concentrations of the two species were roughly equal in the resulting monolayer, future experiments are planned using molecules that are more easily distinguished in STM images. This should allow us to determine the mole fractions of the two species in the adsorbed monolayer. Further studies, which will include other functional groups, differing molecular lengths, and a comparison of the composition of the contacting solution with that of the monolayer will aid in investigating the effects of changing the overlying solution and in exploring the limitations of this technique.

2.6 Conclusions

Alkane monolayers act as templates for monolayers of the identical chain-length ethers, but ether monolayers do not serve as templates for alkane monolayers. The orientation of molecules within a monolayer can be controlled through the use of a monolayer template. The molecules replacing the template layer are more likely to retain the orientation of the template if that orientation offers offsetting favorable interactions.

Table 2.1 Molecular Names, Formulas, and Abbreviations

Name	Formula	Abbreviation
nonacosane	$\text{CH}_3(\text{CH}_2)_{27}\text{CH}_3$	C29
di- <i>n</i> -tetradecylether	$\text{CH}_3(\text{CH}_2)_{13}\text{O}(\text{CH}_2)_{13}\text{CH}_3$	E29
tritriacontane	$\text{CH}_3(\text{CH}_2)_{31}\text{CH}_3$	C33
di- <i>n</i> -hexadecylether	$\text{CH}_3(\text{CH}_2)_{15}\text{O}(\text{CH}_2)_{15}\text{CH}_3$	E33
heptatriacontane	$\text{CH}_3(\text{CH}_2)_{35}\text{CH}_3$	C37
di- <i>n</i> -octadecylether	$\text{CH}_3(\text{CH}_2)_{17}\text{O}(\text{CH}_2)_{17}\text{CH}_3$	E37

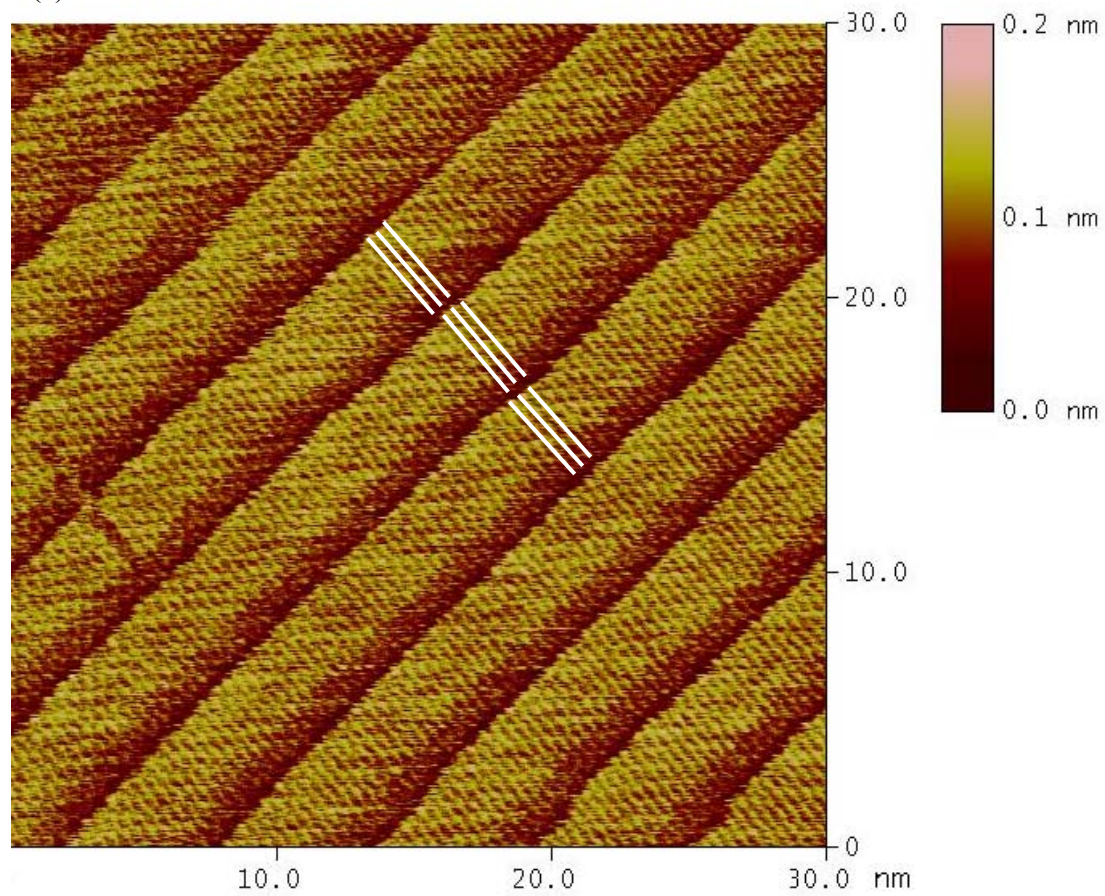
Figure 2.1 Tritriacontane on HOPG

(a) Constant-current STM image of a monolayer of tritriacontane, $C_{33}H_{68}$, adsorbed on a graphite surface. Several molecules are marked by white lines. Imaging conditions were current = 200 pA, $V_{\text{bias}} = 1300$ mV, and sample rate = 30.5 Hz.

(b) A model of a single lamella of an adsorbed tritriacontane monolayer. The molecules are in registry with their molecular axes (dashed arrow) oriented perpendicular to the lamellar axes (solid arrow) giving $\beta = 90^\circ$.

Figure 2.1 Tritriacontane on HOPG

(a)



(b)

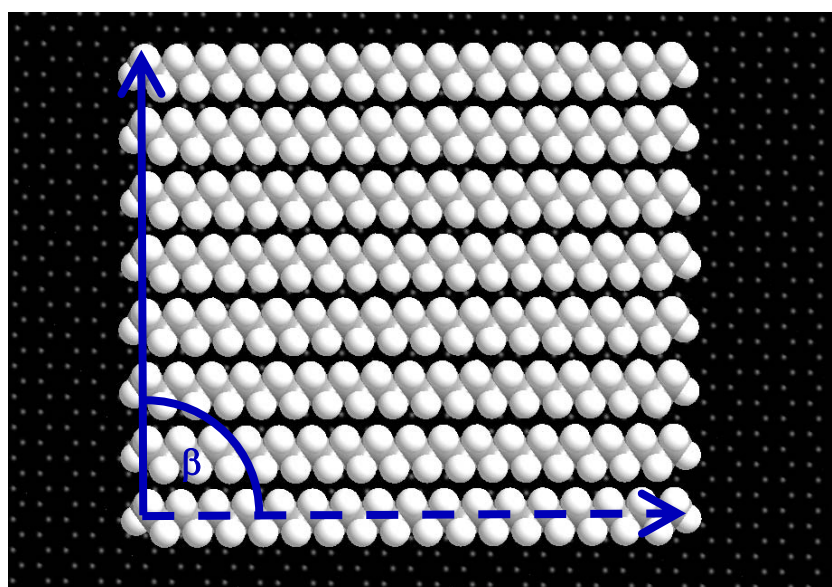


Figure 2.2 Di-*n*-Octadecylether on HOPG

(a) STM image of a monolayer of octadecylether, $\text{CH}_3(\text{CH}_2)_{17}\text{O}(\text{CH}_2)_{17}\text{CH}_3$. Three molecules are marked with white lines. The dark regions appearing in the center of the imaged molecules result from the oxygen atoms. The imaging conditions were $I = 200 \text{ pA}$, $V_{\text{bias}} = 900 \text{ mV}$, and sample rate = 30.5 Hz.

(b) A model of a lamella of an adsorbed octadecylether monolayer. The molecules are offset from registry by two carbons to minimize oxygen-oxygen repulsion. The angle β measures 65° .

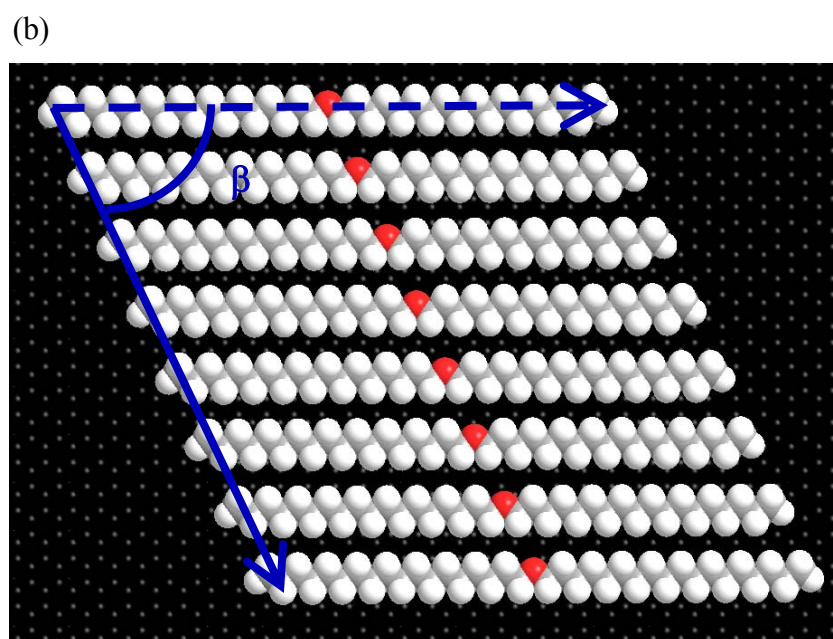
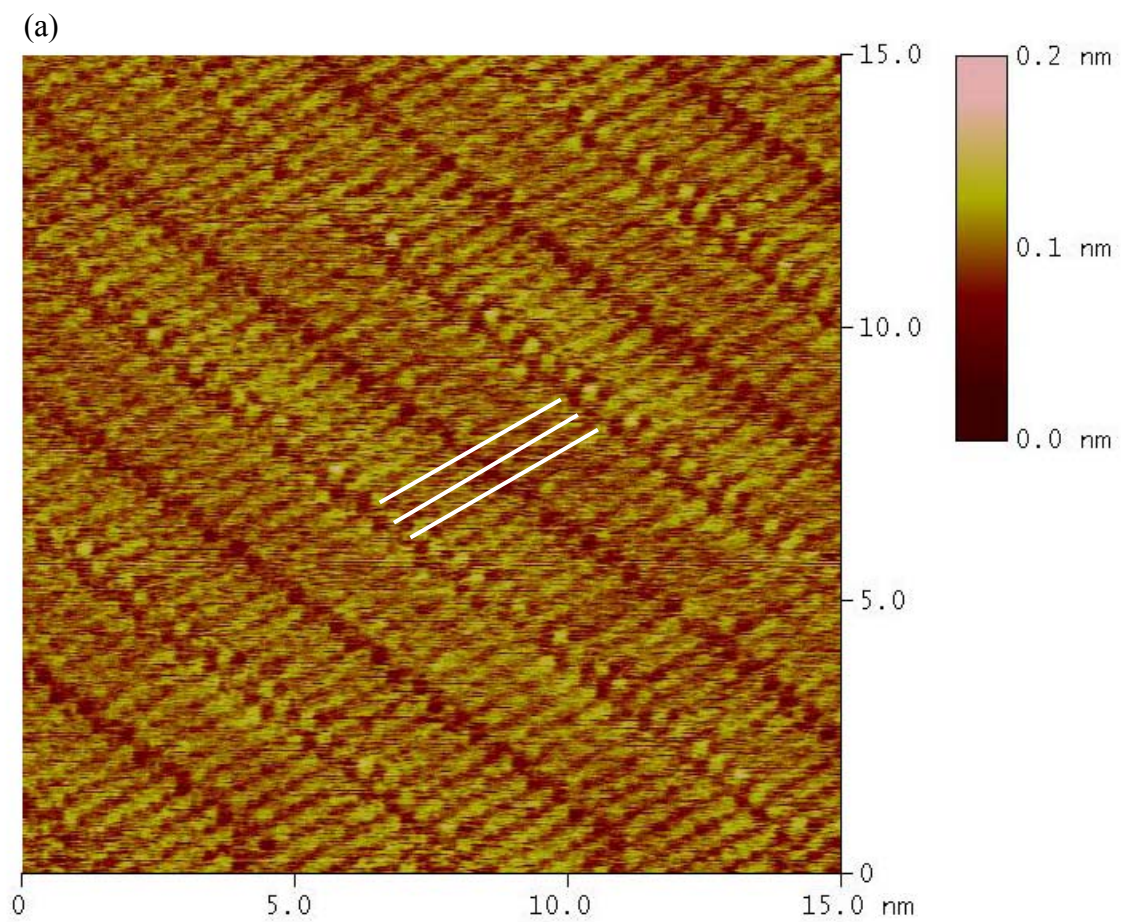
Figure 2.2 Di-*n*-Octadecylether on HOPG

Table 2.2 Measured Monolayer Cell Dimensions

Thermal drift of the STM tip is the principal source of measurement errors. The dimensions are labeled to correspond with those of a crystalline unit cell. Thus a represents the direction along the molecular axis and c represents the direction along the lamellar axis. The length of a single molecule is $a/2$, and c is the distance between adjacent molecules. Literature values from X-ray diffraction are included for comparison purposes: those for the alkanes are from Ref. 25; those for the ether are from Ref. 26.

Table 2.2 Measured Monolayer Cell Dimensions

Molecule	Measurements from STM monolayer images			Literature values for crystals		
	$a/2$ (Å)	c (Å)	β (deg)	$a/2$ (Å)	c (Å)	β (deg)
nonacosane	36.0 ± 0.4	4.1 ± 0.2	88 ± 2	38.760 ± 0.008	4.950 ± 0.001	90
tritriacontane	44 ± 4	5 ± 1	87 ± 3	43.833 ± 0.009	4.995 ± 0.001	90
heptatriacontane	43 ± 3	4.0 ± 0.3	85 ± 4	49.014 ± 0.001	4.957 ± 0.001	90
di- <i>n</i> - tetradecylether	34 ± 2	4.4 ± 0.4	65 ± 4	—	—	—
di- <i>n</i> - hexadecylether	43 ± 3	5.0 ± 0.7	66 ± 6	43.85 ± 0.18	5.57 ± 0.01	63.07 ± 0.32
di- <i>n</i> - octadecylether	44 ± 1	4.6 ± 0.3	65 ± 3	—	—	—

Figure 2.3 STM Image of a Mixed Monolayer of Alkanes and Ethers

A constant-current STM image of a mixed monolayer of tritriacontane and di-*n*-hexadecylether on graphite. The ether molecules can be distinguished by the dark spots in the center of the molecules. Two clusters of ethers are indicated by white arrows. Imaging conditions were $I = 200 \text{ pA}$, $V_{\text{bias}} = 1300 \text{ mV}$, and scan rate = 20.3 Hz.

Figure 2.3 STM Image of a Mixed Monolayer of Alkanes and Ethers

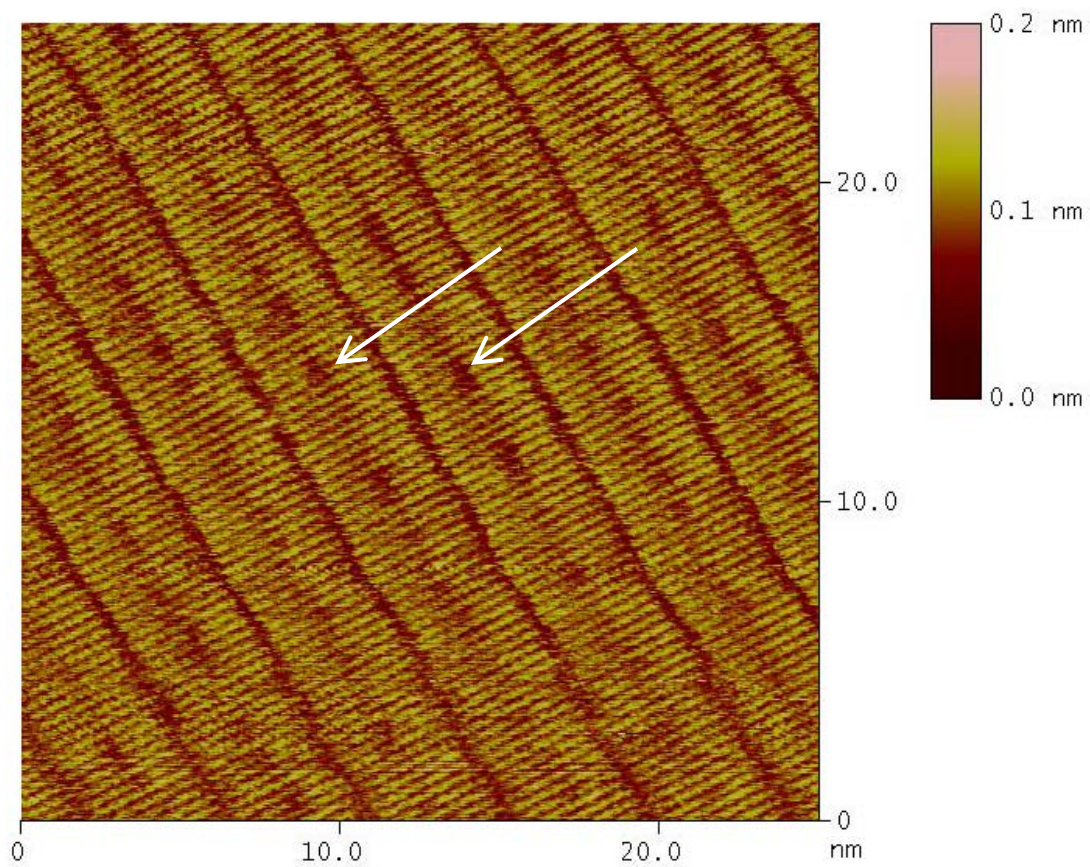
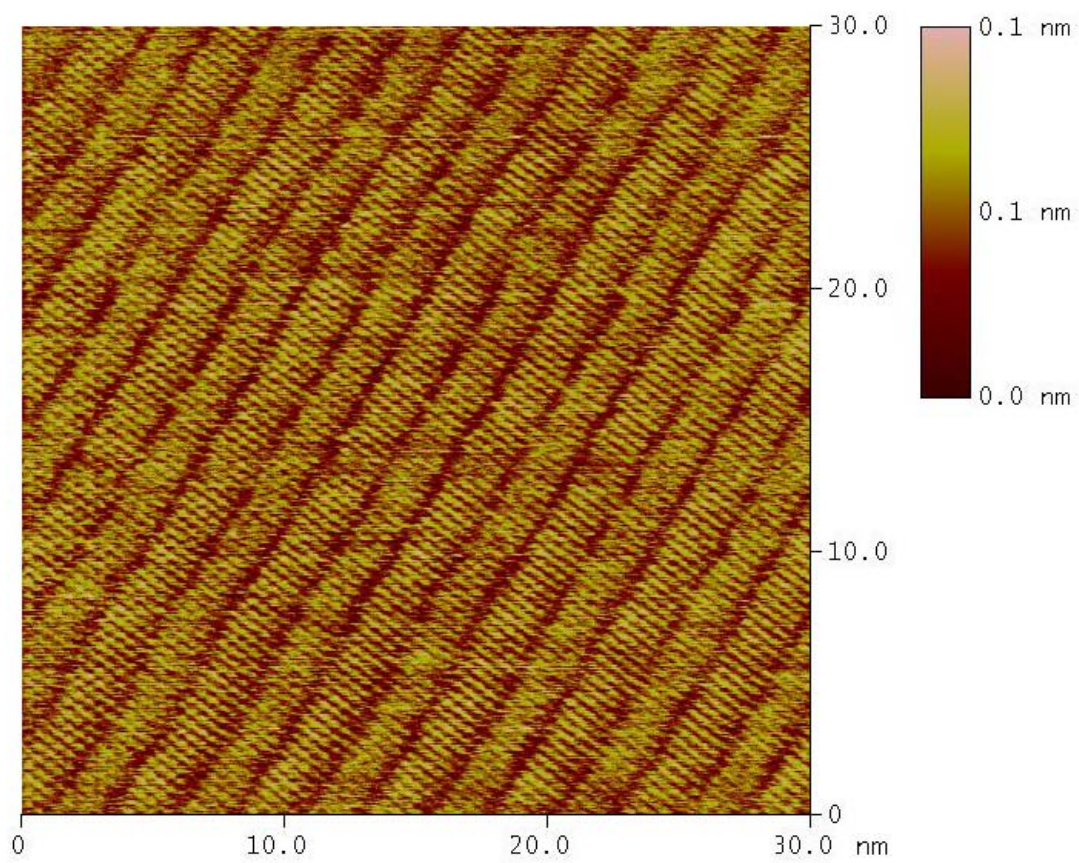


Figure 2.4 STM Image of a Templated Hexadecylether Monolayer

Constant-current STM image of a hexadecylether monolayer formed from a tritriacontane template. The molecules are oriented in the manner typical of alkanes; i.e., with their molecular axes perpendicular to the lamellar axes. The mole fraction of ether in the overlying solution is 0.97. The imaging conditions were $I = 200$ pA, $V_{\text{bias}} = 1400$ Mv, and scan rate = 30.5 Hz.

Figure 2.4 STM Image of a Templated Hexadecylether Monolayer



2.7 References

- (1) Groszek, A. J. *Nature*. **1964**, *204*, 680.
- (2) McGonigal, G. C.; Bernhardt, R. H.; Thomson, D. J. *Appl. Phys. Lett.* **1990**, *57*, 28–30.
- (3) Venkataraman, B.; Flynn, G. W.; Wilbur, J. L.; Folkers, J. P.; Whitesides, G.M. *J. Phys. Chem. B*. **1995**, *99*, 8684–8689.
- (4) Rabe, J. P. and Buchholz, S. *Science* **1991**, *253*, 424–427.
- (5) McGonigal, G. C.; R. H. Bernhardt; Yeo, Y. H.; Thomson, D. J. *J. Vac. Sci. Technol., B: Microelectron. Nanometer Struct. —Process., Meas., Phenom.* **1991**, *9*, 1107–1110.
- (6) Freund, J. E.; Edelwirth, M.; Krobel, P.; Heckl, W. M. *Phys. Rev. B: Condens. Matter Mater. Phys.* **1997**, *55*, 5394-5397.
- (7) Gorman, C. B.; Touzov, I.; Miller, R. *Langmuir* **1998**, *14*, 3052–3061.
- (8) Yin, S. X.; Wang, C.; Xu, Q. M.; Lei, S. B.; Wan, L. J.; Bai, C. L. *Chem. Phys. Lett.* **2001**, *348*, 321–328.
- (9) Yablon, D. G.; Giancarlo, L. C.; Flynn, G. W. *J. Phys. Chem. B* **2000**, *104*, 7627–7635.
- (10) Xie, Z. X.; Xu, X.; Mao, B. W.; Tanaka, K. *Langmuir* **2002**, *18*, 3113–3116.
- (11) De Feyter, S.; Larsson, M.; Schuurmans, N.; Verkuijl, B.; Zorinants, G.; Gesquiere, A.; Abdel-Mottaleb, M. M.; van Esch, J.; Feringa, B.L.; van Stam, J.; De Schryber, F. *Chem.—Eur. J.* **2003**, *9*, 1198–1206.
- (12) Nanjo, H.; Qian, P.; Yokoyama, T.; Suzuki, T. M. *Jpn. J. Appl. Phys., Part 1* **2003**, *42*, 6560–6563.

- (13) Wei, Y. H.; Kannappan, K.; Flynn, G.W.; Zimmt, M. B. *J. Am. Chem. Soc.* **2004**, *126*, 5318–5322.
- (14) Plass, K. E.; Kim, K.; Matzger, A. J. *J. Am. Chem. Soc.* **2004**, *126*, 9042–9053.
- (15) Tao, F.; Goswami, J.; Bernasek, S. L. *J. Phys. Chem. B* **2006**, *110*, 19562–19569.
- (16) Nishino, T.; Buhlmann, P.; Ito, T.; Umezawa, Y. *Phys. Chem. Chem. Phys.* **2001**, *3*, 1867–1869.
- (17) Padowitz, D. F.; Sada, D. M.; Kemer, E. L.; Dougan, M. L.; Xue, W. A. *J. Phys. Chem. B* **2002**, *106*, 593–598.
- (18) Claypool, C. L.; Faglioni, F.; Goddard, W. A.; Gray, H. B.; Lewis, N. S.; Marcus, R. A. *J. Phys. Chem. B* **1997**, *101*, 5978–5995.
- (19) Groszek, A. J. *Nature* **1962**, *196*, 531–533.
- (20) Duim, W. C.; Clarke, S. M. *J. Phys. Chem. B* **2006**, *110*, 23853–23859.
- (21) Padowitz, D. F.; Messmore, B. W. *J. Phys. Chem. B* **2000**, *104*, 9943–9946.
- (22) Stevens, F.; Beebe, T.P. *Langmuir* **1999**, *15*, 6884–6889.
- (23) Kern, H. E.; Piechocki, A.; Brauer, U.; Findenegg, G. H. *Progress in Colloid and Polymer Science* **1978**, *65*, 118–124.
- (24) Claypool, C. L.; Faglioni, F.; Matzger, A. J.; Goddard; Lewis, N. S. *J. Phys. Chem. B* **1999**, *103*, 9690–9699.
- (25) Craig, S. R.; Hastie, G. P.; Roberts, K. J.; Sherwood, J. N. *J. Mater. Chem.* **1994**, *4*, 977–981.
- (26) Kohlhaas, R. *Berichte der Deutschen Chemischen Gesellschaft* **1940**, *73B*, 189–200.

(27) Dorset, D. L.; Clavell-Grunbaum, D.; Snyder, R. G. *J. Phys. Chem. B* **2000**, *104*, 532–537.